ELSEVIER

Comparison of wall spray impaction models with experimental data on drop velocities and sizes

K. Park and A. P. Watkins
Department of Mechanical Engineering, UMIST, Manchester, UK

This paper describes the testing of several spray/wall impaction models developed by the authors and colleagues. A previously unpublished model is described in detail. Most models of spray impaction onto solid surfaces have previously been assessed by comparing the wall spray penetration rates and spray shapes with experimental data. There is a need to establish the ability of models to predict the internal structure of the sprays, because this will influence such parameters as heat transfer and fuel evaporation. Here, therefore, the models are further tested by comparing computer predictions against phase-Doppler anemometry data on spray velocities and drop sizes within the wall spray. The results show that the latest model described here is generally superior to earlier wall impaction submodels in describing these features of the spray. However, the agreement is far from complete, and it is evident that further work is required to enhance the predictive capabilities of the model.

Keywords: wall spray; impaction models; diesel engines; drop velocities

Introduction

The development of compact high-speed direct-injection diesel engines for automobile applications has led to increased interest in the phenomena associated with sprays impacting on solid surfaces. This is not only because of the small size of engine, but also because high-pressure unit injectors are being developed to enable fuel injection quickly in the short time span available at higher engine speeds.

Spray impaction phenomena are difficult to analyse in operating engines because of the problems of access, although useful information can be obtained by, for example, photographic techniques in specially adapted engines, as in Winterbone et al. (1994). However, the details of the data that can be obtained in this way are very limited, and it is difficult to alter the test conditions. For these reasons, most of the recent experimental investigations of impacting sprays have been conducted in specially constructed test rigs or bombs. To make the analysis of results as simple as possible, the "wall" on which the spray is impacted is most often a flat plate. However, both normal and oblique impaction have been studied in this way (Katsura et al. 1989; Senda et al. 1992; Suzuki et al. 1993). Some experiments have also attempted to simulate the effect of swirling flows in engines by incorporating a cross-flowing gas into the rig (Mirza 1991).

In most of these experiments, the main data that have been produced relate to the overall structure of the wall spray subsequent to impaction. Thus is measured the penetration rates of the wall spray and the height or thickness of the spray as it develops along the wall. These are often obtained by photographic means.

Hand-in-hand with the experiments has gone the development of wall impaction submodels for insertion into computer programs. Some of these are of the phenomenological type (Chen and Veshagh 1993), but there have also been developed a number designed for application in multidimensional computational fluid dynamics (CFD) computer codes (Naber and Reitz 1988; Watkins and Wang 1990; Shih and Assanis 1991; Wakisaka et al. 1993, Nagaoka et al. 1994; Park 1994; Bai and Gosman 1995). These submodels have invariably been tested by comparison with the photographs of wall sprays as discussed above and the measurements of wall spray development in terms of penetration and wall spray height, although Bai and Gosman do present some comparisons with drop velocities. These data allow some assessment of the various models to be made. Park presents a new model which appears to provide a better description, over a wide range of engine-like conditions, than do some of the earlier models.

The data discussed above, however, do not provide for a detailed analysis of the internal structure of the wall sprays, in terms of local drop sizes and velocities. The recent work of Arcoumanis and Chang (1994), on the other hand, does provide such detail, by analysing wall sprays at various positions using phase Doppler anemometry (PDA). In this paper, their data are employed to assess the new model of Park (1994) further, and also some earlier models developed by the authors and their colleagues; e.g., Wang and Watkins (1993).

In what follows, the general mathematical description of the gas and spray dynamics, heat transfer, and evaporation are outlined. Subsequently, the new model of Park (1994) is de-

Address reprint requests to A. P. Watkins, Department of Mechanical Engineering, University of Manchester Institute of Science, Manchester M60 1QD, UK.

Received 12 February 1995; accepted 13 March 1996

Int. J. Heat and Fluid Flow 17:424–438, 1996

655 Avenue of the Americas, New York, NY 10010

0142-727X/96/$15.00
PII S0142-727X(96)00049-X

scribed in detail and compared with earlier models developed by the authors and colleagues, and those of Nagaoka et al. (1994) and Bai and Gosman (1995). The test case is then described, and the predicted results of the test case using several of the authors' wall impaction models are compared with experimental data on gas and drop velocities and drop sizes. Finally, conclusions as to the abilities of the various models tested are made and weaknesses in the models are identified.

Mathematical model

The gas phase is modelled in terms of the Eulerian conservation equations of mass, momentum, energy, and fuel vapour mass fraction, and turbulent transport is modelled by the k-ϵ turbulence model in a form for highly compressed flows. The droplet parcel equations of trajectory, momentum, mass, and energy are written in Lagrangian form. Each droplet parcel contains many thousands of drops assumed to have the same size, temperature, velocity components, etc.

The actions of the gas phase on the liquid phase are accounted for through the shear terms in the liquid phase momentum equations and the heat transfer terms in the liquid phase energy and fuel mass conservation equations. The effects of the liquid phase on the gas phase are given as sources or sinks in the mass, momentum, and energy equations of the gas phase. Thus, the two phases are fully coupled, including the evaporation of the liquid phase, although for the test case examined here, the gas and drops are both at room temperature and so evaporation does not occur.

Also included in the model are the drop collision submodels of O'Rourke and Bracco (1980) and the drop breakup submodel of Reitz and Diwakar (1987). The latter model is also used to atomise the spray as it issues from the injector nozzle. The incoming drops are assigned the size of the nozzle diameter. These rapidly break up into 20–30 micron drops a few millimetres downstream.

The approach used here for the solution of these equations is the one developed by Watkins (1989). The gas phase velocity–pressure linkage is handled by the implicit, but noniterative PISO (Issa 1986) algorithm, and the droplet phase equations are integrated into this solution scheme.

In Park (1994) this computational method has been extended to include nonorthogonal computational grids. However, the test case examined in this paper can be adequately handled using orthogonal grids.

The gas phase transport equations are discretised by finite volume means. Within this process, the Euler implicit method is used for the transient term, and a hybrid upwind/central difference scheme is used to approximate the convection and diffusion terms. The ordinary differential Lagrangian equations for the drops are also discretised in the Euler implicit manner.

Wall impaction models

In this paper we examine the wall impaction models developed by Wang (see Watkins and Wang 1990; Wang 1992; Wang and Watkins 1993), as well as the new model from Park (1994).

All these models describe only a small subset of the possible outcome of drops impacting onto a hot or cold surface. Bai and Gosman (1995) identify seven such regimes; namely, (1) "stick," in which drops with little energy impact on a relatively cool surface and remain there in a near spherical state, (2) "spread," in which the drop forms a film on a dry wall or merges with a pre-existing film on a wetted one, (3) "rebound," in which the drop bounces inelastically from the surface, (4) "rebound with break-up," in which the drop breaks up into two or three drops after impacting with a hot surface, (5) "boiling-induced break-up" caused by rapid liquid boiling on a hot surface, (6) "break-up," in which a film is first formed which subsequently disintegrates in a random manner, and (7) "splash," in which the drop impacts at high velocity, forming a liquid crown from which disintegrating jets form.

For most direct injection diesel engines, the wall temperatures are below the critical temperature of the fuel. For such engines, therefore, attention is focused on the rebound, spread, and splash regimes. Models for adiabatic engine calculations undoubtedly need to include the other regimes. Unfortunately, there are little experimental data for surfaces at high temperatures. Recourse must, therefore, be made to low temperature data to validate the models. In that case, the chosen modelled regimes can only approximate the existing regimes. The models of Wang and Watkins (1993) and Park (1994) discussed and tested here are developed for high-temperature surfaces, thus attention is focused on the rebound and break-up regimes. These are used to approximate the rebound and splash regimes of cool surfaces.

Old model

This is the original model developed by Watkins and Wang (1990), which concentrated only on phenomena associated directly with the impaction of single droplets on solid or liquid surfaces. They identified a critical Weber number, where

$$\mathrm{We}_b = \frac{\rho v_{bn}^2 D_{db}}{\sigma}$$

where ρ and σ are the liquid density and surface tension respectively, v_{bn} is the component of the drop velocity normal to the surface just before impact, and D_{db} is the drop diameter then. From experiment (Wachters and Westerling 1966) this number is 80. Thus, the model is divided into two parts. For low We_b, the drops which strike the surface rebound with diminished velocities. At high We_b, the drops shatter into a large number of small drops, some of which rebound from the surface with a small velocity. In this model, the latter phenomenon is ignored. Thus

For $\mathrm{We} < 80$

$$v_{an} = -\alpha v_{bn} \tag{1}$$

$$v_{at} = \alpha v_{bt} \tag{2}$$

$$D_{da} = D_{db} \tag{3}$$

For $\mathrm{We} > 80$

$$v_{an} = 0 \tag{4}$$

$$v_{at} = v_{bt} \tag{5}$$

$$D_{da} = C_{wb} D_{db} \tag{6}$$

Where the subscripts a and b stand for after and before, and t and n represent tangential and normal, respectively. The energy loss coefficient α is calculated from

$$\alpha = \sqrt{1 - 0.95\cos^2\theta} \tag{7}$$

Where θ is the impinging angle to the normal, and C_{wb} is assumed to be $1/3$, so that a drop shatters into 27 equally sized droplets.

Wang's model

Wang (1992) found that the original model was inadequate to obtain the correct development of the wall spray, particularly in

terms of the wall spray thickness, which was severely underpredicted. To overcome this problem, in Watkins and Wang (1990) the collision model of O'Rourke and Bracco (1980) was extended by assuming that droplets after grazing collision will move preferentially in the direction of the local gradient of the void fraction. The velocity after extended grazing collision calculation $\overline{v_{dn}}$ is decided from the following equations:

$$\alpha_n = (1 - \bar{\theta}^b) P\alpha \tag{8}$$

$$\overline{v_{dn}} \cdot (\overline{\mathbf{v}_d} \times \nabla\theta) = 0 \tag{9}$$

$$|\overline{v_{dn}}| = |\overline{\mathbf{v}_d}| \tag{10}$$

Where $\overline{\mathbf{v}_d}$ is the velocity vector of one of the two drops obtained from the original grazing collision model; $\nabla\theta$ is the void fraction gradient; P is a random variable uniform in (0,1); α, α_n are the angles between $\overline{\mathbf{v}_d}$ and $\nabla\theta$, and that between $\overline{\mathbf{v}_d}$ and $\overline{v_{dn}}$, respectively; $\bar{\theta}$ is the average void fraction of all the neighbouring cells; and b is a prescribed constant, set to 1 in the present calculations.

This model is particularly effective in the near wall spray because of large gradients in the local void fraction (or, equivalently, the local liquid volumes). The intention of the model was to disperse the wall spray further away from the wall. Watkins and Wang (1990) and Wang and Watkins (1993) illustrate that this was successfully achieved.

However, it has become apparent that this latter model was implemented incorrectly very near the wall, in that a fictitious "wall" void fraction was employed. In addition, the model was also implemented in the free spray, which results in drops being ejected from the spray, in contradiction to experimental data.

Modified Wang model

In this version of Wang's (1992) model, the near-wall treatment in the extended grazing collision model has been amended to remove reference to fictitious void fractions. And the model has been implemented only where it was designed to be used; i.e., in the wall spray region by requiring that $r > 1.5$ mm, $H < 10$ mm, where r is the radial distance from the spray centreline, and H is measured from the wall.

New model

The model of Park (1994) also uses the data of Wachters and Westerling (1966) to build a wall impaction model. These data are for drops impacting onto a hot surface, above the boiling temperature of the liquid, thus the relevant regimes, as identified by Bai and Gosman (1995), are the rebound, rebound with break-up, break-up, and splash regimes. In the model, only the rebound and break-up regimes are modelled. This model has been applied by Park (1994) and Park and Watkins (1996) to both hot and cold surfaces. As mentioned above, for the latter circumstance, the model is approximating the rebound and splash regimes of cool surfaces, ignoring the spread mode. The transition We_b between the various regimes are also very different for hot and cold surfaces. Wachter and Westerling's data indicate a transition We_b between the rebound and break-up modes of about 80. Bai and Gosman quote a transition between rebound and spread regimes at about We_b of 5. Such a value is probably too low every to occur in engines and in flat plate experiments, except where the wall is placed very far from the injector. Bai and Gosman quote typical values of We_b of 100–400 for impaction in engines and in flat plate experiments where the plate is located less than, say, 30 cm from the injector. These numbers agree with the analyses of the present authors. Thus, the rebound regime would seem not to occur for a wetted wall below the fuel boiling temperature. The transition We_b between the spread and splash regimes is quoted by Bai and Gosman to be given by

$$We_b = 1320 La^{-0.18} \tag{11}$$

where the Laplace number La is defined as

$$La = \frac{\rho\sigma D_{db}}{\mu^2} \tag{12}$$

For the typical values of La quoted by Bai and Gosman (1995), the transition We_b is more than 300. In many experiments, such high values of We_b do not occur, Bai and Gosman quote values of up to 400. Bai and Gosman's results appear somewhat contradictory in that splash velocities are predicted in circumstances where the We_b would seem to be much less than 300.

The rebound model of Park (1994), for $We_b < 80$, is very similar to that of Wang and Watkins (1993), except that the data of Wachters and Westerling (1966) is properly taken into account. Figure 1 shows these data. This curve is digitised and fed into the computer program. For each impacting drop, the We_b is calculated and the We_a obtained from the data. Because there is no change in drop size during impaction, $We_a/We_b = (v_{an}/v_{bn})^2$, and the normal velocity component after impaction is given by

$$v_{an} = -\left(\frac{We_a}{We_b}\right)^{1/2} v_{bn} \tag{13}$$

According to Wachters and Westerling (1966), the tangential velocity component is unaffected by impaction, thus

$$v_{at} = v_{bt} \tag{14}$$

and, finally,

$$D_{da} = D_{db} \tag{15}$$

The break-up model of Park (1994) for $We_b > 80$ is very different from that of Wang and Watkins (1993) and any other model so far published. It is based on Wachters and Westerling's (1966) data of the spreading of the liquid film about the central dome as a drop deforms on impact on a hot solid or liquid surface, Figure 2. Figure 2(a) shows the drop about to impact on the surface with normal velocity v_{bn} at time $t = 0$. The velocity of

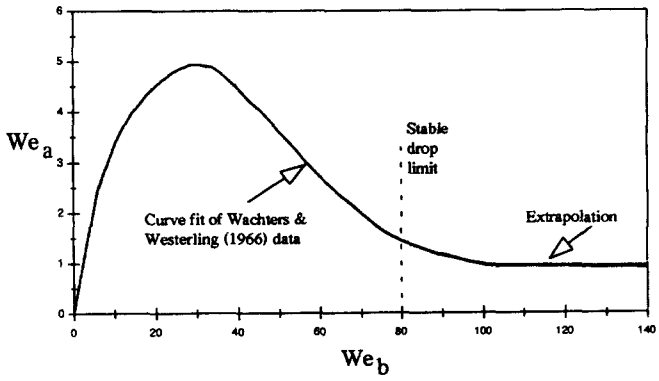

Figure 1 Relationship between Weber numbers at arrival and departure

the liquid in the drop is assumed to remain the same until the dome, as shown in Figure 2(b), entirely disappears. This agrees with the data of Stow and Hadfield (1981) who show that there is little deviation from the initial drop velocity. Thus, this happens at $t = t^* = D_{db}/v_{bn}$. The liquid film continues to spread outwards, with radius r_f and average film thickness h_f, as shown in Figure 2(c). The data of Wachters and Westerling were analysed by Park (1994) to obtain an equation for r_f as follows.

$$r_f = 0.835\left[3.096\frac{t}{t^*} - \left(\frac{t}{t^*}\right)^2\right]D_{db} \tag{16}$$

From mass conservation, the film thickness h_f is obtained from

$$h_f = \frac{D_{db}^3}{6r_f^2} \tag{17}$$

At the moment the dome disappears, $t = t^*$, $r_f^* = 1.75D_{db}$ and $h_f^* = 0.0544\ D_{db}$. The maximum value of r_f is $r_{f\max} = 2D_{db}$, at $t = 1.548t^*$. The equivalent $h_{f\min} = 0.0417D_{db}$.

Now h_f would appear to be the characteristic size of droplets resulting from the break-up of the film. However, for typical values of D_{db} of 20–30 μm, h_f^*, for example, is 1.1–1.6 μm. From experimental evidence of drop break-up on cool surfaces, such droplet sizes are far too small; see, e.g., Mundo et al. (1995). Instead, it is envisaged that drops impacting on cool, wetted surfaces will spread out with a wave motion, involving fluid already on the surface, as shown experimentally by Yarin and Weiss (1995). The amplitude of these waves would be much larger than the values of h_f deduced above.

To obtain drop sizes after break-up, therefore, the data of Naber and Farrell (1993) is employed. They showed that, over the range of We_b examined, up to 120, the number of droplets N resulting from the break-up of a single drop impacting on a hot surface is a linear function of We_b. These data have been analysed by Park (1994) to give

$$N = 0.187We_b - 14.0 \tag{18}$$

Although there is no experimental evidence to justify it, this correlation has been used for higher values of We_b, up to about 500 in this paper, and for even higher values in Park (1994) and Park and Watkins (1996).

Bai and Gosman (1995) also give a linear function of N on We_b, as

$$N = 5.0\left(\frac{We_b}{We_c} - 1\right) \tag{19}$$

based on the data of Stow and Stainer (1977). For the transition We_c, evaluated above as more than 300, this equation becomes $N \approx 0.016\ We_b - 5.0$.

Clearly, there is a large discrepancy between the two datasets, which results in the droplet sizes predicted by Equation 18 being about half that for Equation 19. Mundo et al. (1995) found size distributions for the splashed droplets, as a function of $K = We_b^{1/2}Re_b$, where Re_b is the Reynolds number, based on the normal velocity component on impact, over a range of We_b from 620 to 1182. If attention is focused on the peak values of these distributions, then values of N can be approximately deduced as a function of We_b. Although this is not a linear function, the actual values of N agree more closely with those from Equation 18, than Equation 19. A similar conclusion can be drawn from the data of Yarin and Weiss (1995). The computations presented later shed more light on the correctness or otherwise of Equation 18.

The equations given above on droplet sizes and numbers give the diameter ratio D_a/D_b as proportional to $We_b^{-0.333}$ for large values of We_b. This is in close agreement with the data and model of Nagaoka et al. (1994), who found this diameter ratio to be proportional to $We_b^{-0.36}$.

In Park's (1994) model the impacting drop is assumed on average to retain its original tangential velocity component after impaction. This is in agreement with the data of Mundo et al. (1995). But also the droplets after break-up have an additional component, calculated from Equation 16, as follows.

The edge of the film propagates radially outwards from the impaction site with a velocity v_f, given by

$$v_f = \frac{dr_f}{dt} = 0.835\left(\frac{3.096}{t^*} - \frac{2t}{t^{*2}}\right)D_{db} \tag{20}$$

Insertion of $t^* = D_{db}/v_{bn}$, yields

$$v_f = 0.835\left(3.096v_{bn} - 2v_{bn}^2\frac{t}{D_{db}}\right) \tag{21}$$

Now the film is most likely to break-up between the times $t = t^*$, and $t = 1.548t^*$ when the drop would otherwise start to shrink up again. Suppose the break-up occurs at $t = \chi t^*$, where $1.0 \le \chi \le 1.548$, then

$$v_f = 0.835(3.096 - 2\chi)v_{bn} \tag{22}$$

Droplets which result from the break-up would have a range of this additional velocity from zero, at the centre of the impaction site, to v_f, at the film edge. However, selection of a large number of droplets with a wide range of different velocities would quickly result in the swamping of the storage capacity of

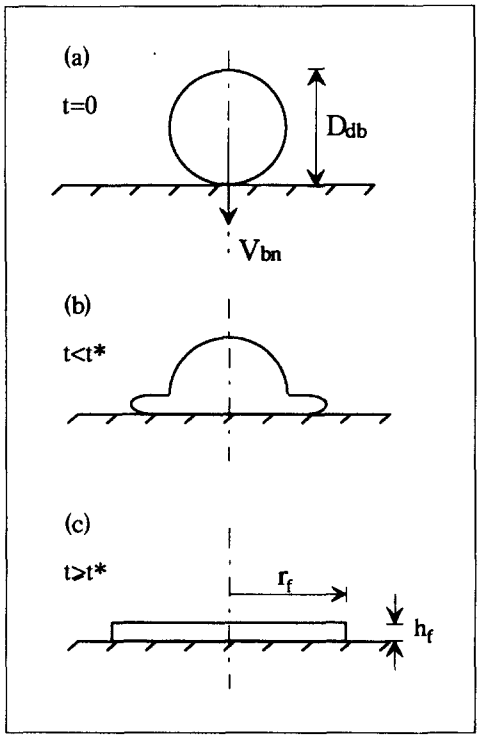

Figure 2 Deformation of impacting drop

even the largest computer. Instead here, as done also by Bai and Gosman (1995), two representative droplets are chosen. These two droplets are treated separately by Bai and Gosman. However, Park (1994) chose to give the new droplets the same sizes, but with opposite sign on the additional tangential velocity calculated from Equation 22, by multiplying by a random number R_{xx} in the range (0,1). Thus, the droplet tangential velocities after break-up are given by

$$v_{at} = v_{bt} \pm R_{xx} v_f \tag{23}$$

The actual value of χ has been subjected to some analysis by comparing the predicted rate of spread of wall sprays on flat walls against experimental data over a wide range of conditions, Park (1994). It was found that, on average, for sprays impacting at reasonably large distances from the injector; e.g., 30 cm, where impaction velocities are of the order of $v_{bn} = 10$–20 m/s, then a value of $\chi = 1.0$ was satisfactory. However, for impaction very close to the injector, Park (1994) and Park and Watkins (1996), where impaction velocities may be an order of magnitude higher, $\chi = 1.28$ was found to be optimal. The directions in which the new droplets move are determined by selecting an angle randomly in the range $(0, 2\pi)$.

The normal velocity component of the droplets after break-up are obtained from the tail of the Wachters and Westerling (1996) curve, Figure 1. Thus, a uniform value of $We_a \approx 1.0$ is assumed for $We_b > 100$. The number of droplets N is calculated as specified above, then from mass conservation $D_{da} = D_{db}/N^{0.333}$. Finally the normal velocity component is calculated from

$$v_{an} = -\left(\frac{\sigma We_a}{\rho D_{da}}\right)^{0.5} \tag{24}$$

Mundo et al. (1995) found that the normal velocity component of ejected drops is sharply distributed about 0.208 v_{bn} for smooth walls and 0.407 v_{bn} for rough walls. This is for normal impaction. Thus, the v_{an} would appear to be dependent on $We_b^{0.5}$. However the range of values of $K = We_b^{0.5} Re_b$ investigated was small. Insertion of typical values of We_b in Mundo et al.'s data would indicate considerably higher values of v_{an} than in the present model, deduced from Wachter and Westerling's (1966) data. Nagaoka et al. (1994) also indicate an order of magnitude higher values of We_a than found from that data. Thus, the extrapolation from the hot wall data into the cool wall condition is not valid for this aspect of the model. That this is a weak point in the present model is demonstrated in the test case later.

Note that all the original drop is assumed to be divided into the new droplets; i.e., no liquid is left on the surface. The present model does not calculate adhered liquid, although this component of the model of Bai and Gosman (1995), for example, could easily be adapted. Alternatively, the present model describes the situation where the adhered mass has reached a steady-state condition.

Test case

The test case employed here is one of these described by Arcoumanis and Chang (1994). A single diesel spray was injected normally onto a flat unheated aluminium plate, at a vertical distance of 30 mm from the orifice. A total of 4.0 mm^3 was injected, following the injection profile shown in Figure 3. The conditions were atmospheric; i.e., pressure = 1.013 bar, and temperature = 288 K. At these conditions, it is possible to employ PDA to simultaneously measure droplet velocities and sizes. The

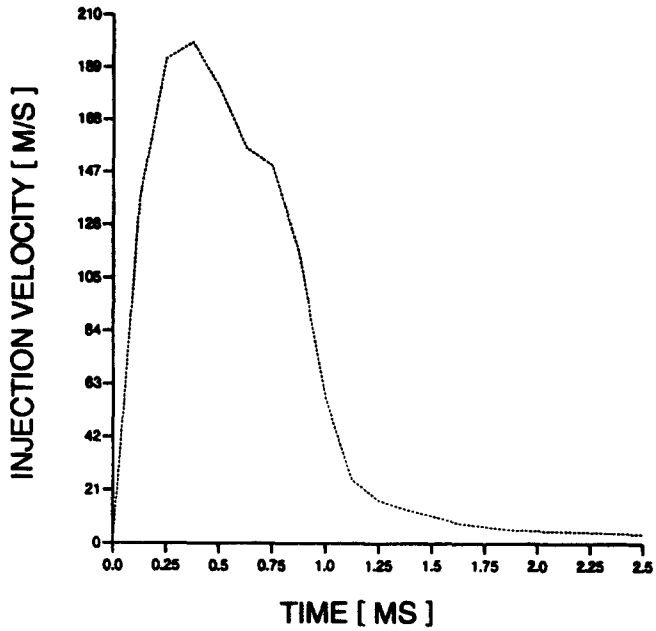

Figure 3 Injection velocity curve

measurement locations are shown in Figure 4. These allowed the flow in each of the main regions of the wall spray to be investigated.

A 35 × 35 line grid is used for the simulation, as shown in Figure 5. Here the injector is at the top left and injecting downwards towards the wall at the bottom. The grid is made denser near the wall in order to better resolve the wall spray.

For the calculations shown here, a time step of 3 μs is used. During the injection period a total of 4000 drop parcels are introduced. This was limited by the storage capacity of the computer employed. As will be seen later, there are not enough droplets in some parts of the spray to claim statistically independent results.

Results and discussion

The test case above was simulated four times, each time only the wall impaction model was varied. The four models employed are those described above. The old model of Watkins and Wang (1990) is denoted by OLD in the figures to follow. The model including the extended grazing collision model (Watkins and Wang 1990; Wang and Watkins 1993) is denoted by WANG(ORI). The modified version of the model is denoted by WANG(MOD). And the new model of Park (1994) is denoted by NEW.

At three points in the spray flow, Arcoumanis and Chang (1994) measured the mean flow velocity development with time. The chosen points were at (1) $r = 10$ mm, $H = 3.0$ mm, (2) $r = 10$ mm, $H = 5.0$ mm, and (3) $r = 15$ mm, $H = 5.0$ mm. As can be seen from Figure 5, for much of the time point (1) is on the border between the main wall-jet region and the stagnation region. Point (2) is definitely in the stagnation region. Point (3) is in the wall-jet vortex, for much of the later time recording was made.

The PDA measures the movement of drops, hence the experimental data are those of droplet velocities. It could be assumed that, because the only gas motion is that induced by spray, then the gas motion would closely follow the drop velocities, at least in those areas where drops have resided for a substantial period. The models predict differing amounts of dispersion of the drops away from the wall after impaction. Some of the models fail to

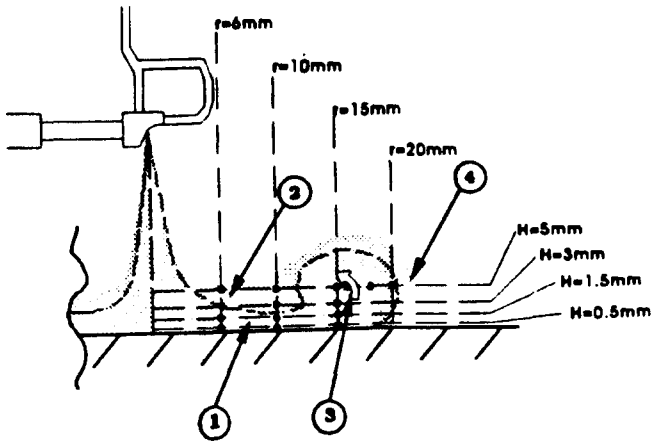

(1) Main Wall-Jet Region (3) Wall-Jet Vortex
(2) Stagnation Region (4) Leading Edge

Figure 4 Measuring locations

predict any drops existing at one or more of the three points above. So we have chosen to plot gas phase velocities at all these points in Figures 6–8. This method allows the predicted structure of the entire wall jet, including both air and spray drops, to be assessed.

Figure 6 shows the results returned by each of the four wall impaction models at point (1), compared to the experimental data. The times appended to the vectors indicate the elapsed time since injection started. According to the experiment, after about 0.6 ms, the first spray drops pass through the measurement position, moving almost parallel to the wall. However, as the spray develops, the point in question first becomes part of the head vortex, so that the velocity vector swings upwards away from the wall, then downwards again, as the head vortex passes by. Finally, the vector attains a steady-state position in which the flow is directed almost vertically downwards towards the wall. Clearly, at this point, for times greater than 2.0 ms after the start of injection, the flow has reached a quasi-steady state in which air is essentially being entrained into the main wall-jet region.

The model predictions at this point show that the spray arrives significantly earlier than measured. The overpenetration of the early predicted wall spray is probably due to the lack of dispersion of the spray away from the wall. Thus, more momentum resides in the spray near the wall. For all the models, with the exception of Wang's (1992) original model, the velocity vector swings around, as in the experiment. Wang's model predicts that the vector starts to move in an anticlockwise manner, but after 0.9 ms, it starts to swing back clockwise again. It is difficult to see that this could be the correct behaviour. It is thought that this may be due to interference from drops ejected from the free spray by the incorrect imposition there of the extended grazing model of Wang. The results from all the other three models are very similar. The motion is too slow in the 0.8–1.1 ms elapsed time period, suggesting that the air entrainment into the actual spray is more vigorous than that predicted. This has the effect of pushing the head vortex past the measurement position more quickly than predicted. The underlying failing here is probably again the lack of dispersion of the predicted spray leading to less momentum transfer to the surrounding air above the spray, once the main body of the spray has passed by. For all the models, the time taken for the vector to settle to a steady-state position agrees well with the experiment, and the direction of the steady-state motion also agrees well. There are significant differences in the strength of the velocity, denoted by the lengths of the vectors. Again, this is likely to be determined by the spray distribution. The modified Wang model appears to capture this feature the best.

The experimental data and the corresponding predictions are shown in Figure 7 for point (2). The measured development here is similar to that at point (1), except that the rotation takes

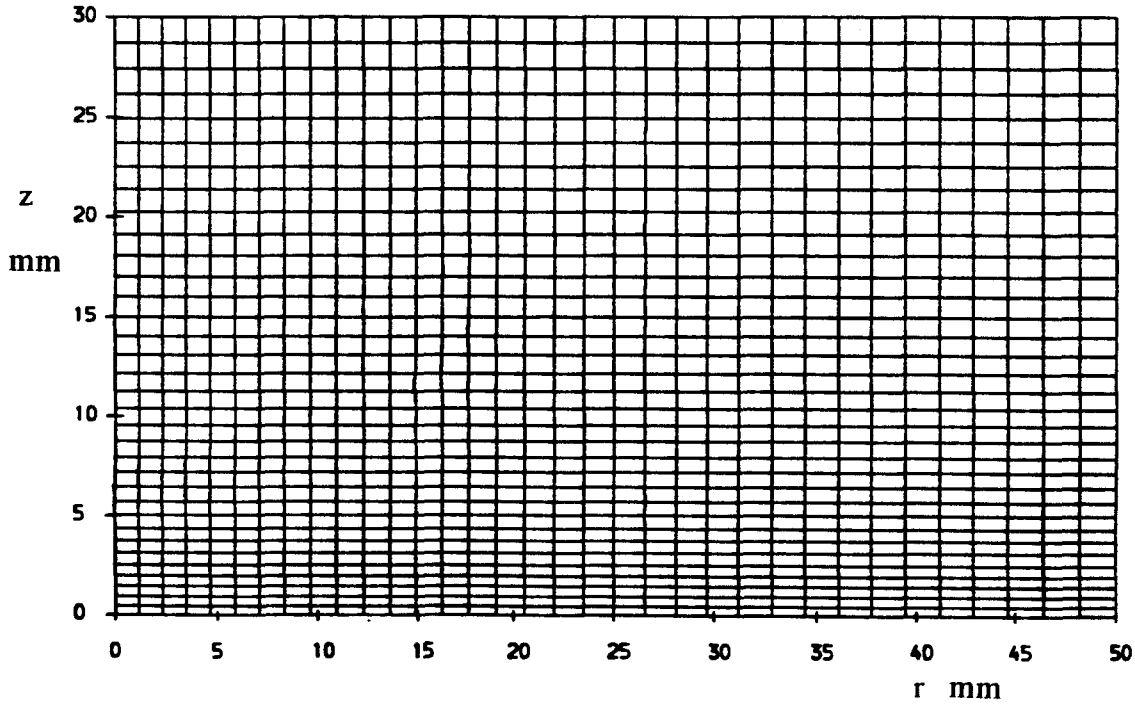

Figure 5 Computational grid

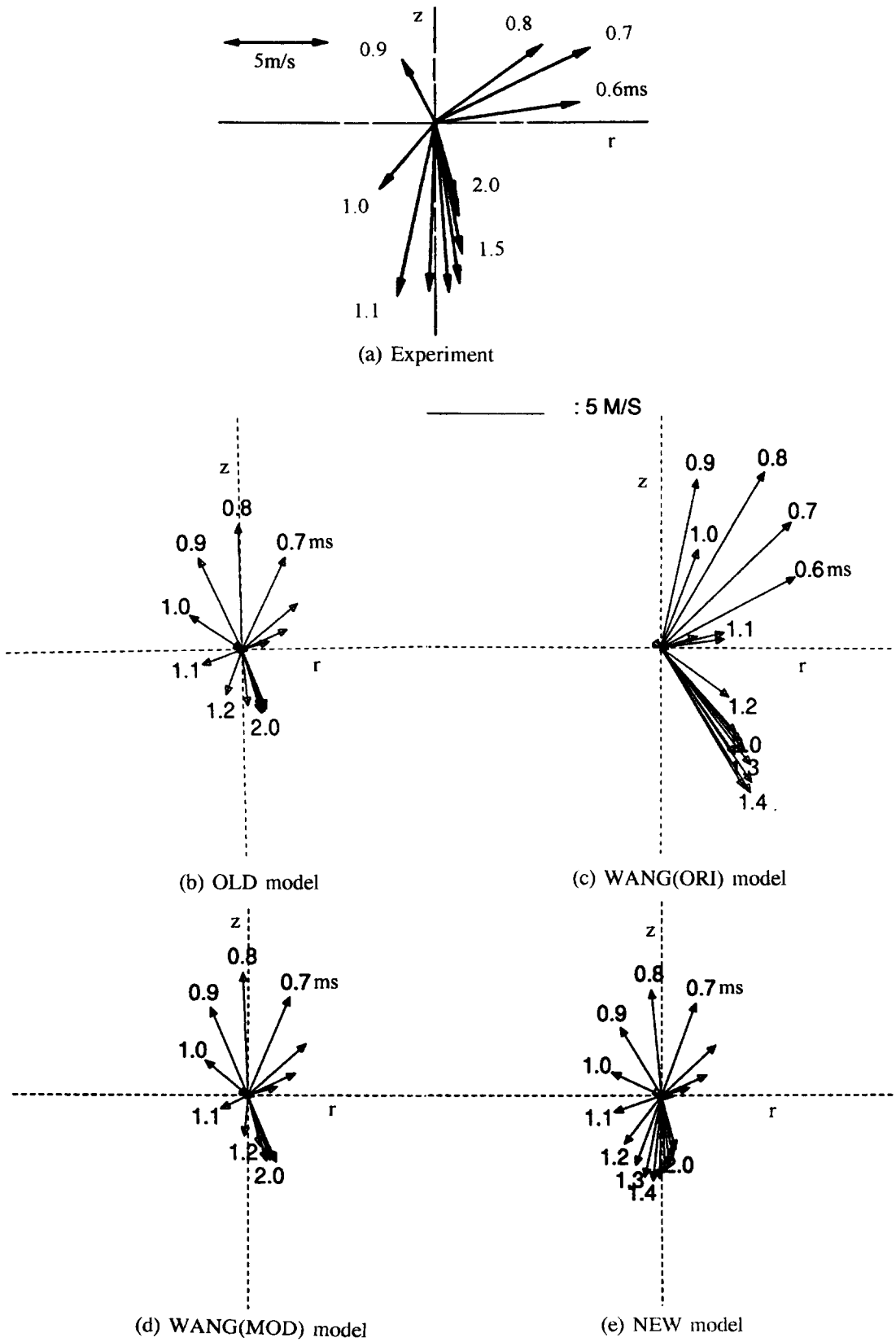

Figure 6 Experimental and predicted flow velocities at point (1)

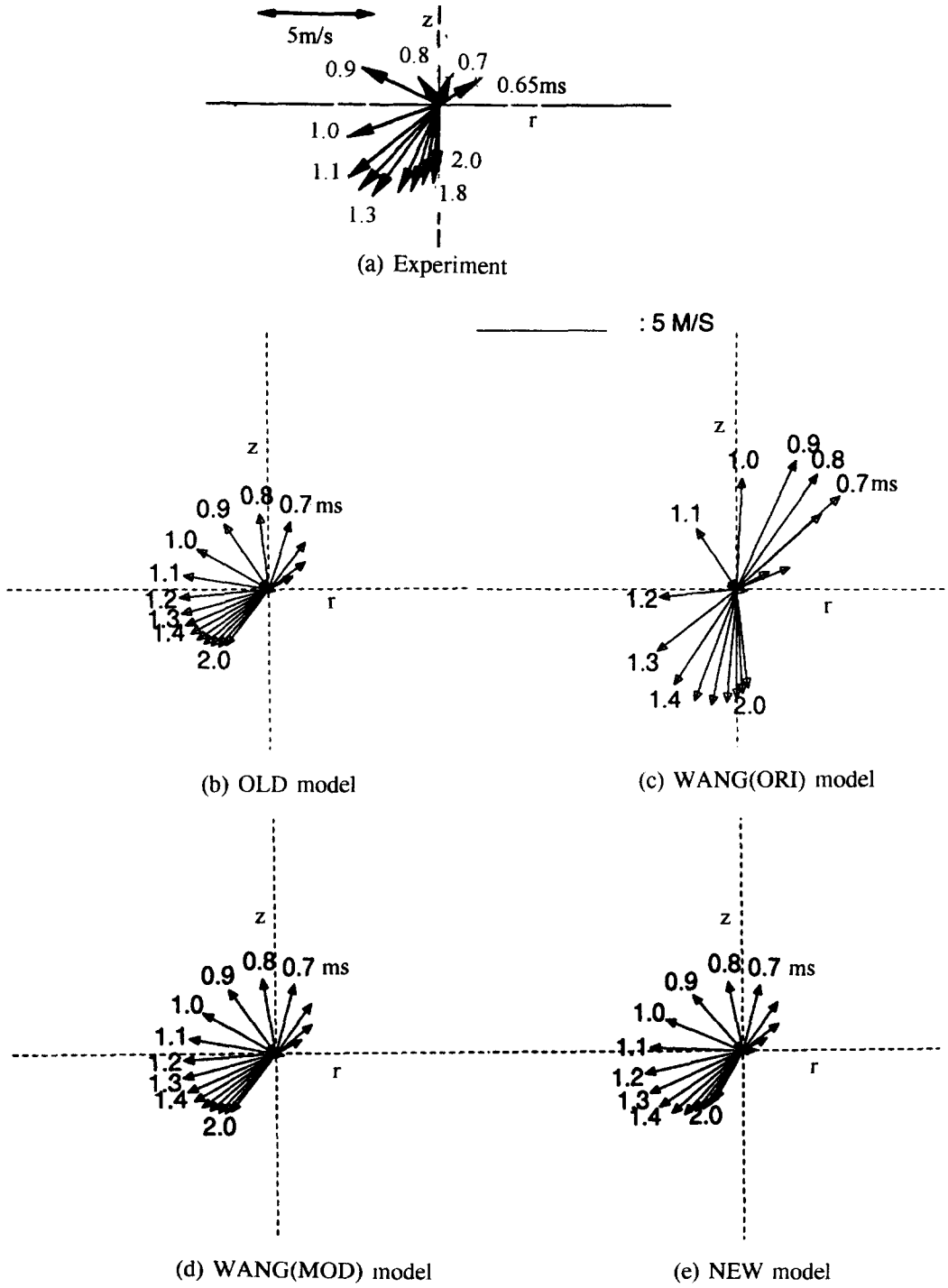

Figure 7 Experimental and predicted flow velocities at point (2)

slightly longer and the velocities are significantly reduced. Both of these features are captured by all the models. However, the models predict too slow a rotation rate with the original Wang (1992) model being particularly slow. The steady-state direction is predicted to be at an angle of between 30° and 45° to the vertical, except for the original Wang model, which gives almost perfect agreement for this feature. The flow at this point is particularly sensitive to the spray dispersion, because the point lies very near the outer edge of the wall spray. Any underprediction of the spray dispersion must cause large changes in the velocity values and directions. The original Wang model predicts the greatest dispersion, hence the good agreement with experimental data.

The development of the flow at the final point (3) is shown in Figure 8. Here the data indicate that the steady-state position may not have been reached over the 2.3 ms time span shown. However, the same rotation of the flow is evident as for the first two points. This starts rather later than those two points, because

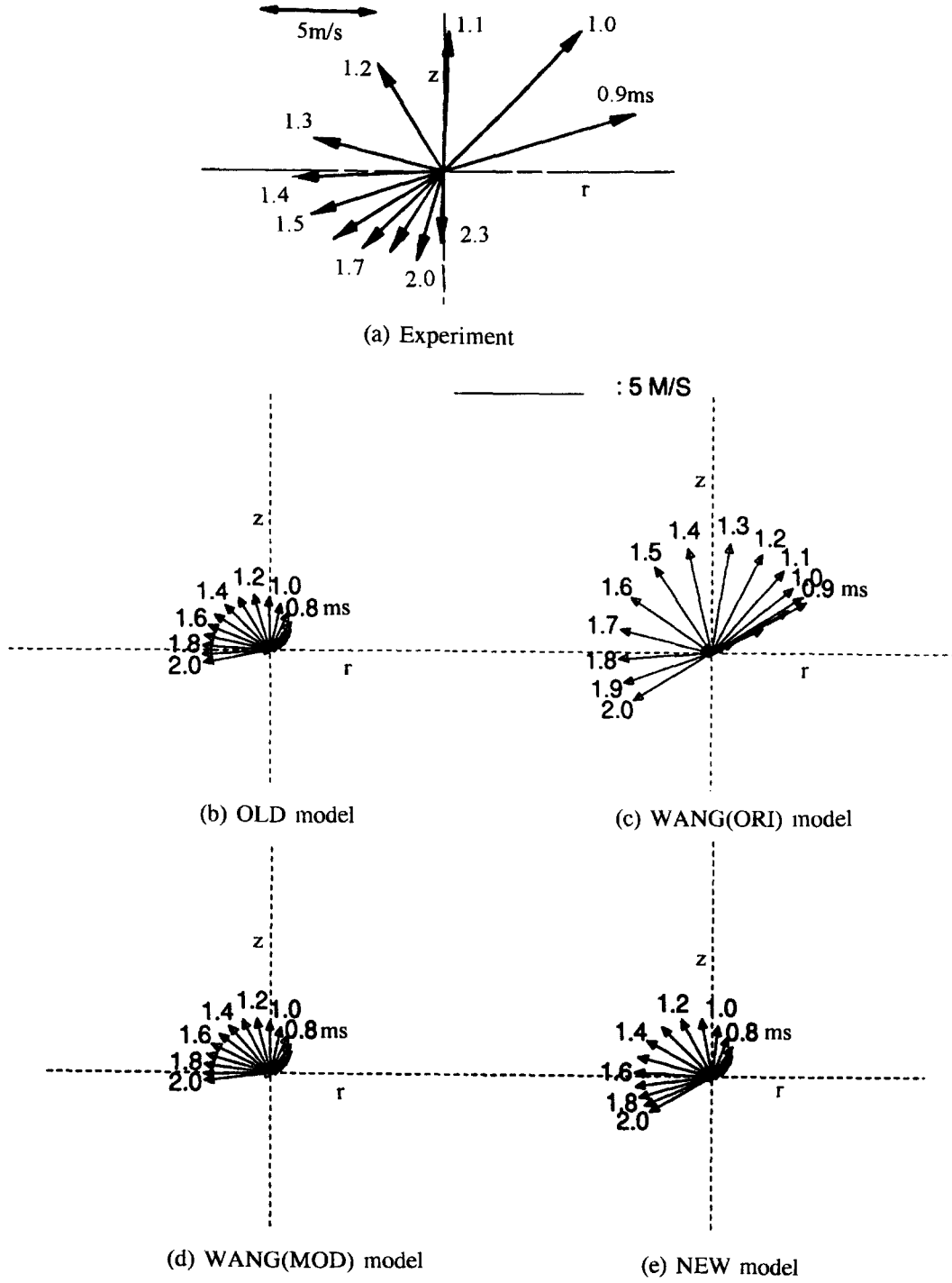

Figure 8 Experimental and predicted flow velocities at point (3)

the spray takes longer to reach this point at $r = 15$ mm. The velocity vectors are considerably larger than for point (2) during the early development. The reasons for this are difficult to understand, because this point is further from the impingement point and the spreading out of the spray would imply reduced velocities. None of the models gives the correct flow development in time for this point. Predictions from the models indicate that the flow is directed back towards the origin of the wall spray even after 2.0 ms. Calculations were stopped at this point in time, so it is not known if these models eventually would also predict downwardly directed flow. The new model and the original Wang (1992) model give the best development, although the latter is again slow. The strength of the velocities are only predicted well by the original Wang model. This point is at $H = 5$ mm, the same as point (2). It would appear that the same deficiencies in the models as cited there produce even poorer predictions here. This may be because of the reduced momentum of the spray drops as the spray flows radially outwards.

The tangential (along the wall) components of the drops velocities were measured at a larger number of points, as indi-

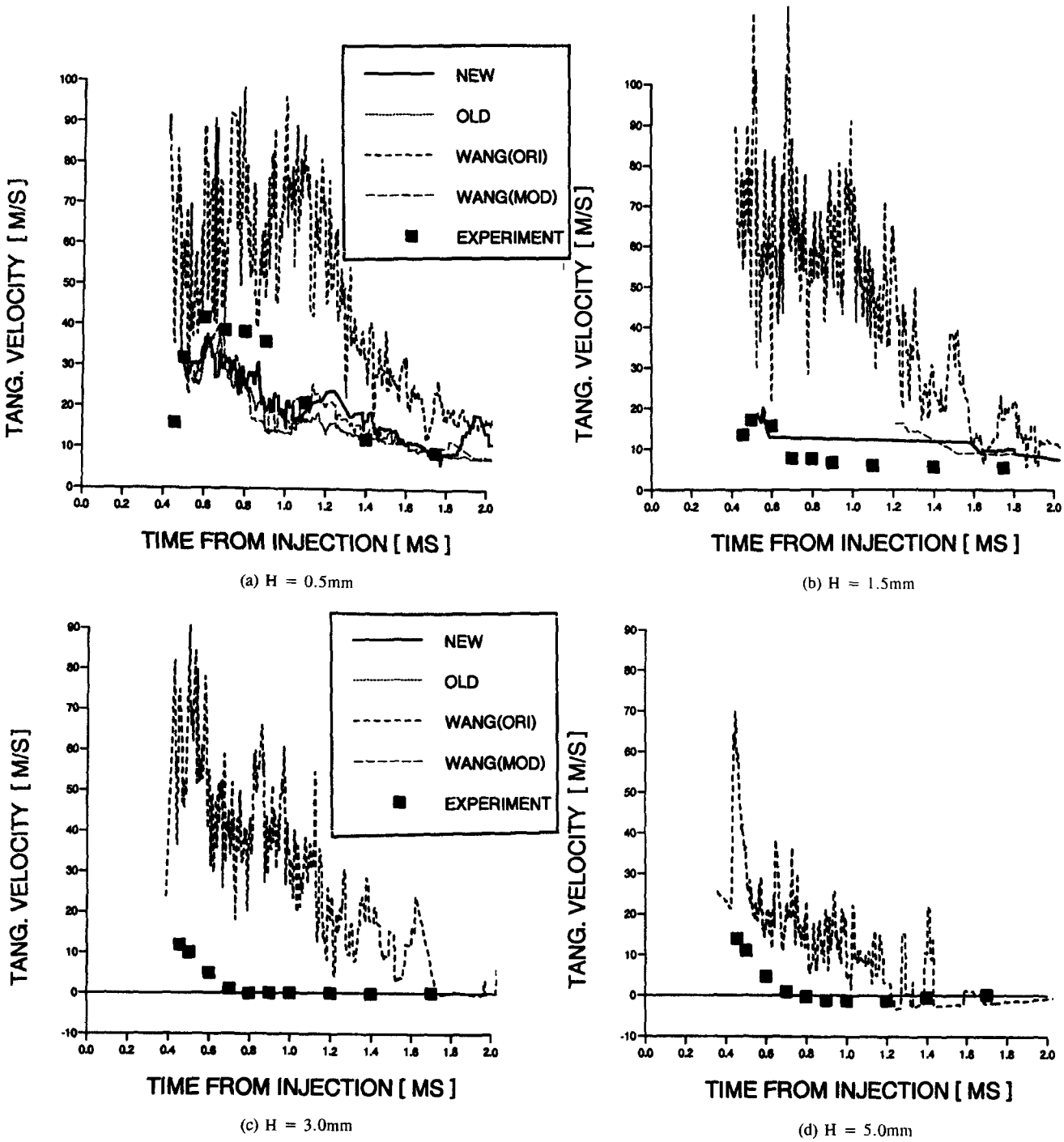

Figure 9 Experimental and predicted tangential velocities at $r = 6$ mm

cated in Figure 4. These are plotted in Figures 9–11 for radial positions $r = 6.0$, 10.0, and 15.0 mm, respectively, and for distances from the wall of $H = 0.5$, 1.5, 3.0, and 5.0 mm. Also plotted on these figures are the predicted results for the four wall impaction submodels. These are now droplet velocities, hence there are gaps in the results at points where the drops have not reached, or reach later than in the experiment, or indeed disappear from again later.

The predicted values are obtained by an ensemble of data from drops within a 1 mm cube centered at the point in question. The dimensions of the cube are set as a compromise between the facts that if the cube is too small, then insufficient drops will be present in the cube to obtain a statistically meaningful average, and that if the cube is too large, then spatial smearing of the data may occur. The reason for the oscillations in the predicted results presented in Figures 9–12 is that too few drop parcels were present in the control volume to obtain a proper ensemble of data.

At the $r = 6$ mm locations (Figure 9), which are closest to the impaction area of the spray (but outside the free spray region)

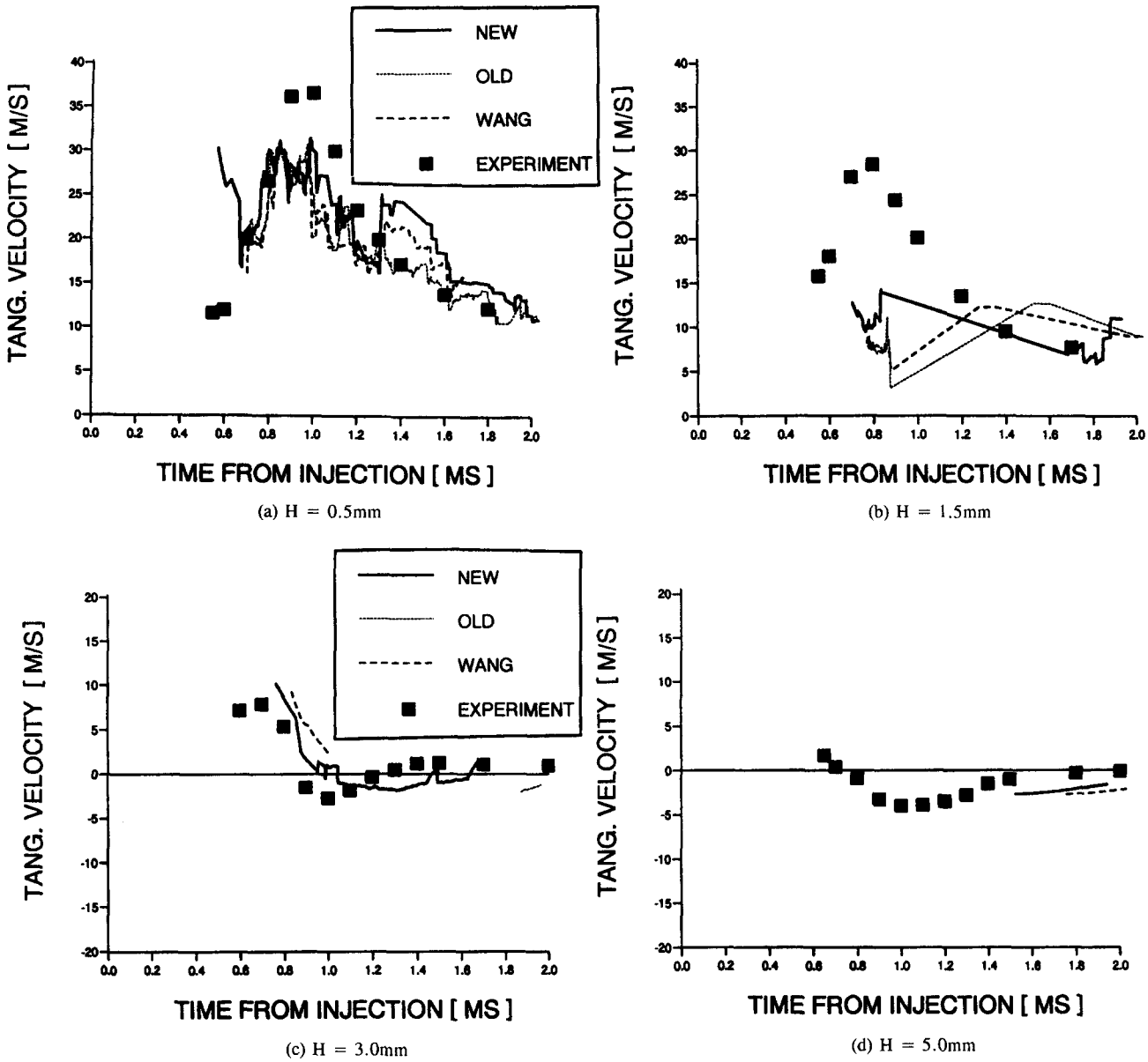

Figure 10 Experimental and predicted tangential velocities at $r = 10$ mm

the measured tangential velocity rises abruptly to relatively high values near the wall, before gradually diminishing as the initial spray passes through. The near-wall velocities have not settled to a quasi-steady state within the time span of the experiment, but those further from the wall have done so. For values of H equal to or greater than 3.0 mm, this steady-state velocity is zero. Hence, it would appear that the spray here is either stationary or does not exist after about 0.8 ms.

Spray is predicted by all four models at $H = 0.5$ mm, but not at $H = 1.5$ mm by the old model of Wang (1992), nor by the modified Wang model before 1.2 ms. This is because of the zero normal velocity component assigned to the drops after impaction at higher We_b values. This prevents dispersion of the drops away from the wall. Application of the extended collision model of Watkins and Wang (1990) obviously does not completely alleviate this problem. Only the original Wang model predicts drops at $H = 3.0$ mm and $H = 5.0$ mm. However, this latter model substantially overpredicts the tangential component of the drop velocity. This is because these drops are those which were ejected from the free spray by employment of the extended collision model there.

It is shown by Park (1994) that the normal droplet velocity component is also too high with this model, resulting in sprays which are too dispersed away from the wall. Clearly, employment of the extended grazing collision in the free spray is distorting the results of the wall spray treatment. This model also gives erroneous results for the tangential velocities at all the other measuring locations. For this reason, this model will no longer be considered here. The modified Wang model, which also employs the extended collision model, but only in the wall spray, does not result in drops appearing in these larger H positions.

It is evident that, where the old, new, and modified Wang models predict the existence of drops, these models give a greatly superior prediction of the tangential velocity component than

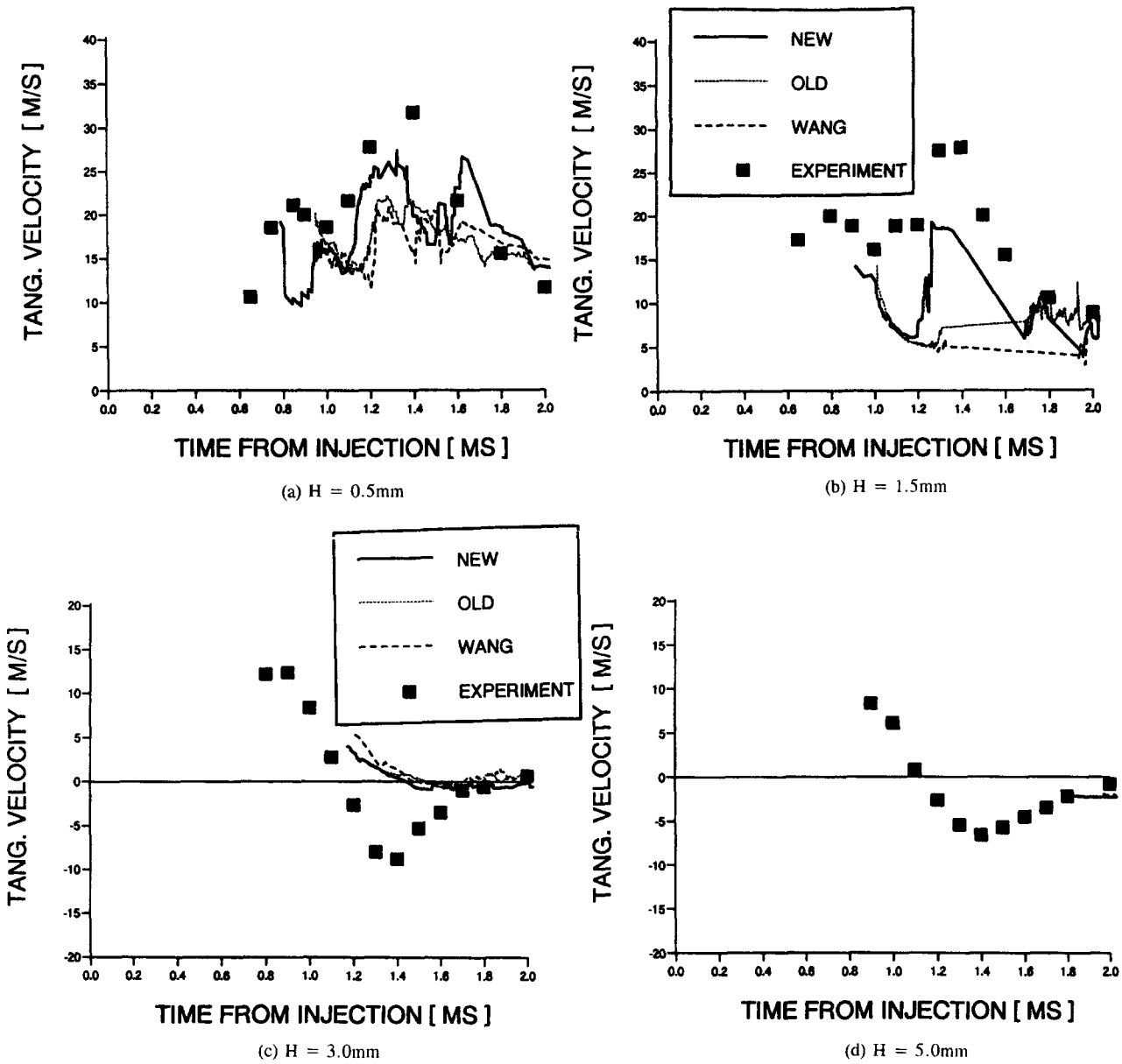

Figure 11 Experimental and predicted tangential velocities at $r = 15$ mm

does the original Wang (1992) model. All these models correctly predict the abrupt initial rise to a peak velocity, followed by the gradual fall. There is little to choose between the model results at $H = 0.5$ mm, but the new model gives the best results at $H = 1.5$ mm. The lack of dispersion of the droplets even for the new model, is evident at $H = 3$ and 5 mm. Clearly, larger values of normal velocity components of droplets after impingement at high We_b are required.

The measured situation at $r = 10$ mm is similar to that at $r = 6.0$ mm, as shown in Figure 10, except that the initial rise to a peak velocity value is more gradual and the peak value at $H = 1.5$ mm is substantially higher. For the positions $H = 3.0$ mm and $H = 5.0$ mm, negative velocities appear, as illustrated in Figures 6 and 7.

At the near-wall measurement location, all three models give good predictions for the data, although the early flow predictions around 0.6 ms using the new model give a second spurious peak in the tangential velocity component with no obvious physical explanation. The old model gives the best description of the decay process. Further away from the wall at $H = 1.5$ mm, the agreement is substantially worse with peak velocities only 40% of those measured. The predicted values are very similar to those at $r = 6$ mm, $H = 1.5$ mm. One explanation is that the high momentum spray near the wall is not sufficiently convected away from the wall to this position, because the normal velocity components are too small. Only the new model gives the correct trend with time. At $H = 3.0$ mm, the new model is the only one to return negative velocity components. This is in contrast to the gas phase predictions shown in Figure 6. For the other two models, drops appear only briefly in this position. Thus, the new model gives a substantial advantage over the modified Wang model, even though the latter is applying the extended collision model in order to disperse drops further away from the wall. At $H = 5.0$ mm, the modified Wang model also produces negative velocities only after about 1.8 ms. Again, this is in clear contrast to the gas velocities shown in Figure 7. Once again, the lack of dispersion

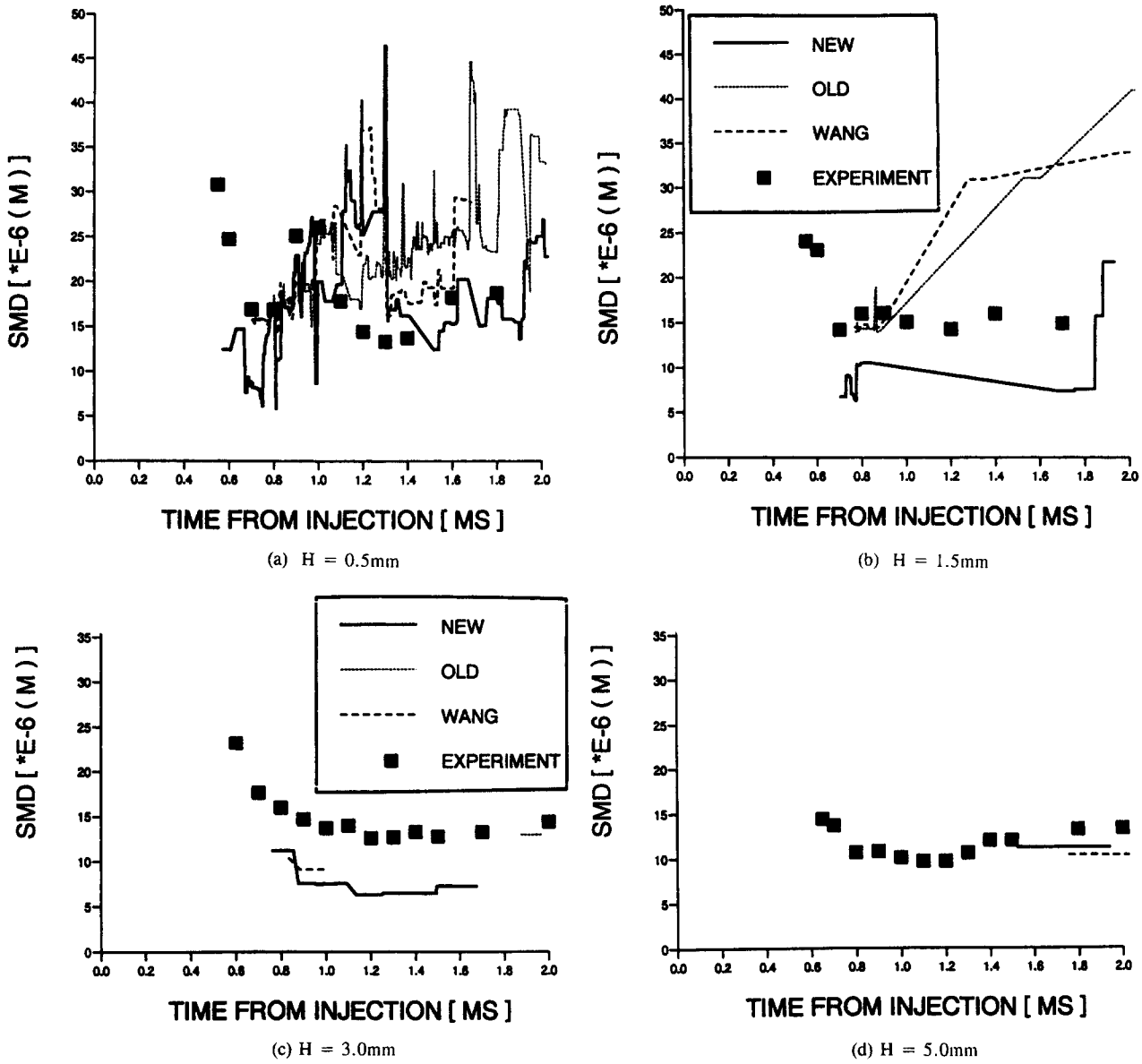

Figure 12 Experimental and predicted SMDs at $r = 10$ mm

of the droplets due to too small normal velocities after impingement is probably to blame.

Finally, in Figure 11, are shown the results at $r = 1.5$ mm. The experimental data show a quite different variation of the tangential velocities at these locations. For the near wall positions, $H = 0.5$ and 1.5 mm, there is an initial low peak, followed by a second higher peak as the head vortex passes through. For the $H = 3.0$ mm and 5.0 mm locations, the initial peak velocity is followed by an equally large dip, as the head vortex drives the droplets back towards the origin of the wall spray.

At the near-wall location, $H = 0.5$ mm, the main variations in tangential velocity are captured by all the models. Perhaps the best results are returned by the new model, although early on, around 0.8–1.0 ms, and later, beyond 1.6 ms, the variations are incorrect. The predictions are considerably worse at the $H = 1.5$ mm position. The new model roughly captures the correct variation, but errors are large. Neither of the other two models capture the second peak. The predictions, however, are considerably improved over the same H position at $r = 10$ mm. This is because of the spray development which allows more higher-momentum drops to disperse further away from the wall. All the models settle down to approximately the correct velocity value towards the end of the spray. At $H = 3.0$ mm, all the models predict some negative velocity component. Even then, this occurs approximately 0.4 ms too late, and the magnitude of the velocity is much too small. However, the general variation of the results are correct. At $H = 5.0$ mm, both the new model, when it predicts droplets, and the modified Wang model return negative tangential velocity values. However, these are again too little and occur far too late. This is again due to the lack of droplets appearing in the predictions at these positions.

The PDA system is capable of simultaneous droplet velocity and size measurements. The latter data are characterised by the Sauter Mean Diameter (SMD). Figure 12 shows the measured and predicted variations at the $r = 10$ mm measurement locations. The overall trend of the experimental data is for the drop sizes to decrease sharply during the early development of the wall spray and then to decrease more gradually in the middle

stage. Finally, there is a very gradual rise again towards the end of the measuring time. The former phenomenon may be due to the initial burst of larger drops at the head of the spray being followed by smaller drops and drops which have broken up on impact with the surface. The SMD evolution at the near-wall location is more oscillatory than elsewhere. This may be due to the effects of droplet collisions amongst the thick spray near the surface which form larger drops. Once this first burst of drops has passed through, the drop sizes fall again, only to be followed by a second gradual increase in drop sizes. This latter trend is due to the decreased approach velocities of the free spray towards the end of the injection period. This decrease in velocity results in a reduced breakup of the drops on the wall.

Figure 12 shows that the impaction submodels also follow these trends. They also give SMDs of drop sizes which are close to the 10–25 mm measured by the PDA system. Although far from perfect, the new model gives the variations in SMD at $H = 0.5$ mm which best matches the data, both in variation and value. The oscillations in the predictions here result from rapid changes in drop sizes due to the effects of drop collisions and breakup. There are probably too few droplets passing through the measuring location to smooth out these variations. At $H = 1.5$ mm, the SMD variations are not well predicted, although generally the new model gives the best results. It is probable that the initial burst of large droplets are confined in the predictions to a thin layer of less than 1.5 mm above the wall. This is ascribed to the too small normal velocities of the splashed droplets. As a result, the SMDs are underpredicted by 30–40%. The old and Wang models give the wrong variation here and result in drop sizes which are more than 100% too large at the end of the measuring period.

Further away from the wall at $H = 3.0$ mm, the new model give a good predictions of SMD variation, but at about 50% of the measured values. At $H = 5.0$ mm, the new model and the modified Wang model predict the presence of drops only very late in the injection for reasons described above. The level of agreement on size is better than that at $H = 3.0$ mm.

Overall the new model gives a substantially better description of the measured SMD values and variations than do any of the earlier models. In the near-wall region, $H = 0.5$ mm the values of SMD returned by the new model match the measured values well. This suggests that the drop break-up submodel, Equation 18, does give an accurate description of this phenomenon, and that the model of Bai and Gosman (1995) might well give droplet sizes which are too large. This has not been tested by Bai and Gosman. The model tends to give smaller droplets further away from the wall. This may be due to aerodynamic break-up of the drops, but it is more likely that the majority of these drops are small drops which did not impact on the wall but were diverted by the action of the larger drops and entrained gas forming the main body of the wall spray. Because of the underestimation of the normal velocity components of the relatively larger splashed droplets, these do not progress outwards into the higher layers of the spray, and thus the SMD of the droplets is too low there.

From the above examination of the predicted results, it is clear that none of the models assessed here provides a very good overall description of the wall spray. It is clear that the extended collision model, when applied only in the wall spray region, does disperse the drops away from the wall and generally gives a better description of the tangential velocities, and particularly the drop sizes, than does the old model of Watkins and Wang (1990). However, the level of dispersion is inferior to that given by the new model of Park (1994). A weak link in all the Wang models is the prescription of a constant to describe the break-up of drops on impaction. Adjustment of this could bring the result of the modified Wang model better into line with the measured drop sizes, as is seen with the Park model.

As for the two models which do not employ the extended grazing model, the new model is clearly superior to the old model. The latter, in particular, fails to predict drops at locations quite close to the wall. Where both models predict the presence of drops, the new model gives superior predictions of both tangential velocities and drop sizes.

A major weakness of the Park (1994) model is the reliance on data from conditions for which the model is not strictly applicable. It would appear that there is sufficient data for cool wall situations to allow adequate models to be built for at least some of the prevailing impaction regimes, as done for example by Bai and Gosman (1995). However, for hot wall situations, further data are needed. This particularly applies to the break-up and splash regimes, where data on normal velocities and drop sizes after impaction are needed in order to complete and validate the model.

Conclusions

In this paper, a single experiment has been simulated. The conditions are atmospheric, and, therefore, the conclusions may not pertain to engine-like conditions. However, for the conditions examined, the following conclusions can be drawn.

(1) The original Watkins and Wang model (1990) is not suitable for wall spray calculations if the extended collision model is employed in the free spray as well as the wall spray. The wall spray is distorted by drops ejected from the free spray.

(2) If the extended collision model is employed only in the wall spray region, the wall spray is dispersed better, but much less than with the original Wang (1992) model.

(3) The new model of Park (1994) gives a better shape to the wall spray than the modified Wang model, and gives better agreement on tangential velocities and drop sizes, expressed through the Sauter Mean Diameter, than any of the other models. Still, there are regions of the spray, as determined experimentally, in which the new model does not predict drops.

(4) Park (1994) shows that the new model also gives a better description of wall sprays, than does the Wang and Watkins model (1993) and the Wakisaka et al. model (1993), for more engine-like conditions. These include high pressures and temperatures. Further cases of high pressure and temperature calculations where the impaction velocities are very high, also show the superiority of the new model over that of Naber et al. (1988).

(5) However, Park's (1994) model is based on experimental data obtained from drops impacting on a hot surface, above the boiling point of the liquid, but is being used here for impaction on a cool surface. As a consequence, the model cannot perform very well. To some extent the position is alleviated by using additional data which pertain to the cool wall situation. The main weakness of the model is in the prescription of the normal velocity components of droplets after impaction. These are clearly much lower in the hot wall experiments of Wachters and Westerling (1966), than for cooler walls, as in, e.g., Mundo et al. (1995). For cool wall situations, the model could therefore be substantially improved by adopting the latter data to select normal velocities after impaction. On the other hand, the data of Wachters and Westerling, adopted here, on tangential velocities, appears to give a reasonable description of this aspect of the wall spray.

(6) For Park's (1994) model to be useful in both hot and cold wall situations, it clearly needs to divide more neatly between the two situations, rather than the current mixture. That the data exists for the cool wall situation has been illustrated here and by, for example, Bai and Gosman (1995), despite

some criticisms expressed here. However, further data on the hot wall situation are needed, particularly of normal velocity components for the break-up and splash regimes, and droplet sizes after impaction.

References

Arcoumanis, C. and Chang, J. C. 1994. Flow and heat transfer characteristics of impinging transient diesel sprays. SAE 940678

Bai, C. and Gosman, A. D. 1995. Development of methodology for spray impingement situation. SAE 950283

Chen, C. and Veshagh, A. 1993. A simple unified fuel spray model. SAE 930923

Issa, R. I. 1986. Solution of the implicitly discretised fluid flow equations by operator-splitting. *J. Comp. Phys.*, **62**, 40–65

Katsura, N., Saito, M., Senda, J. and Fujimoto, H. 1989. Characteristics of a diesel spray impinging on a flat wall. SAE 890264

Mirza, 1991. Studies of diesel spray interactions with cross-flows and solid boundaries. Ph.D. Thesis, University of Manchester, Faculty of Technology, Manchester, UK

Mundo, C., Sommerfeld, M. and Tropea, C. 1995. Droplet-wall collisions: Experimental studies of the deformation and breakup process. *Int. J. Multiphase Flow*, **21**, 151–173

Naber, J. D., Enright, B. and Farrell, P. 1988. Fuel impingement in a direct injection diesel engine. SAE 881316

Naber, J. D. and Farrell, P. 1993. Hydrodynamics of droplet impingement on a heated surface. SAE 930919

Naber, J. D. and Reitz, R. D. 1988. Modelling engine spray/wall impingement. SAE 880107

Nagaoka, M., Kawazoe, H. and Nomura, N. 1994. Modelling fuel spray impingement on a hot wall for gasoline engines. SAE 940525

Park, K. 1994. Development of a non-orthogonal-grid computer code for the optimisation of direct-injection diesel engine combustion chamber shapes. Ph.D. thesis, University of Manchester Institute of Science and Technology, Manchester, UK

Park, K. and Watkins, A. P. 1996. An investigation of combustion chamber shapes for small automotive direct injection diesel engines employing spray impaction. Accepted by Proc. I. Mech. E., J. of Automobile Engineering

O'Rourke, P. J. and Bracco, F. V. 1980. Modelling of drop interactions in thick sprays and a comparison with experiment. Stratified Charge Automotive Conf. IMechE.

Reitz, R. D. and Diwakar, R. 1987. Structure of high pressure fuel sprays. SAE 870598

Senda, J., Fukami, Y., Tanabe, Y. and Fujimoto, H. 1992. Visualization of evaporative diesel sprays impinging upon wall surface by exciplex fluorescence method. SAE 920578

Shih, L. K. and Assanis, D. N. 1991. Implementation of a fuel spray wall interaction model in KIVA-II. SAE 911787

Stow, C. D. and Hadfield, M. G. 1981. An experimental investigation of fluid flow resulting from the impact of a water drop with an unyielding dry surface. *Proc. R. Soc. Lond. A*, **373**, 419–441

Stow, C. D. and Stainer, R. D. 1977. The physical products of splashing water drops. *J. Meteorol. Soc. Japan*, **55**, 518–531

Suzuki, M., Nishida, K. and Hiroyasu, H. 1993. Simultaneous concentration measurement of vapour and liquid in an evaporating diesel spray. SAE 930863

Wachters, L. H. J. and Westerling, N. A. J. 1966. The heat transfer from a hot wall to impinging water drops in a spheroidal state. *Chem. Eng. Sci.*, **21**, 1047–1056

Wakisaka, T., Yoshida, S. K., Isshiki, Y. and Shimamoto, Y. 1993. A study on spray models for numerically analysing fuel spray behaviour. *Proc. 11th Symposium on Internal Combustion Engines*, JSME/JSAE, 241–246 (in Japanese)

Wang, D. M. 1992. Modelling spray wall impaction and combustion processes of diesel engines. Ph.D. thesis, University of Manchester, Faculty of Technology, Manchester, UK

Wang, D. M. and Watkins, A. P. 1993. Numerical modelling of diesel wall spray phenomena. *Int. J. Heat Fluid Flow*, **14**, 301–312

Watkins, A. P. 1989. Three-dimensional modelling of gas flow and sprays in diesel engines. In *Computer Simulation of Fluid Flow, Heat and Mass Transfer and Combustion in Reciprocating Engines*, N. C. Markatos (ed.), Hemisphere, Bristol, PA, 193–237

Watkins, A. P. and Wang, D. M. 1990. A new model for diesel spray impaction on walls and comparison with experiment. *Proc. COMODIA 90 Int. Symposium on Diagnostics and Modelling of Combustion in I.C. Engines*, Kyoto, Japan, 243–248

Winterbone, D. E., Yates, D. A., Clough, E., Rao, K. K., Gomes, P. and Sun, J. H. 1994. Quantitative analysis of combustion in high-speed direct injection diesel engines. *Proc. COMODIA 94 Int. Symposium on Diagnostics and Modeling of Combustion in I.C. Engines*, Yokohama, Japan, 261–267

Yarin, A. L. and Weiss, D. A. 1995. Impact of drops on solid surfaces: Self-similar capillary waves, and splashing as a new type of kinematic discontinuity, *J. Fluid Mech.*, **283**, 141–173